Nat. Hazards Earth Syst. Sci. Discuss., 2, 5171–5212, 2014
www.nat-hazards-earth-syst-sci-discuss.net/2/5171/2014/
doi:10.5194/nhessd-2-5171-2014

Natural Hazards and Earth System Sciences
Open Access
Discussions

Floods in the Niger basin – analysis and attribution

V. Aich[1], B. Koné[2], F. F. Hattermann[1], and E. N. Müller[3]

[1]Potsdam Institute for Climate Impact Research, Potsdam, Germany
[2]Wetlands International, Mali Office, Mopti, Mali
[3]Institute of Earth and Environmental Science, University of Potsdam, Potsdam, Germany

Received: 8 July 2014 – Accepted: 24 July 2014 – Published: 14 August 2014

Correspondence to: V. Aich (aich@pik-potsdam.de)

Published by Copernicus Publications on behalf of the European Geosciences Union.

Abstract

This study addresses the increasing flood risk in the Niger basin and assesses the damages that arise from flooding. Statistics from three different sources (EM-DAT, Darthmouth Flood Observatory, NatCat Munich RE) on people affected by floods show positive trends for the entire basin beginning in the 1980s. An assessment of four subregions across the Niger basin indicates even exponential trends for the Sahelian and Sudanian regions. These positive trends for flooding damage match up to a time series of annual maximum discharge (AMAX): the strongest trends in AMAX are detected in the Sahelian and Sudanian regions, where the population is also increasing the fastest and vulnerability generally appears to be very high. The joint effect of these three factors can possibly explain the exponential increase in people affected by floods in these subregions. In a second step, the changes in AMAX are attributed to changes in precipitation and land use via a data-based approach within a hypothesis-testing framework. Analysis of rainfall, heavy precipitation and the runoff coefficient shows a coherent picture of a return to wet conditions in the basin, which we identify as the main driver of the increase in AMAX in the Niger basin. The analysis of flashiness (using the Richards–Baker Index) and the focus on the "Sahel Paradox" of the Sahelian region reveal an additional influence of land-use change, but it seems minor compared to the increase in precipitation.

1 Introduction

In the last two decades, the occurrence of extensive flooding has increased drastically in the Niger basin (Amogu et al., 2010; Descroix et al., 2012; Mahe et al., 2013; Panthou et al., 2014); however, very little research is currently being conducted on both factors contributing to flood risk and the associated flood damages. Tarhule (2005) addressed the flooding in the Sahel for the first time scientifically, calling the floods "the other Sahelian hazard" referring to the lesser significance of floods in the face of the dominant water scarcity in the region. Since then, several studies have contributed to the discussion from different perspectives.

Paeth et al. (2011) looked at the meteorological patterns that lead to the extreme flooding of 2007. Panthou et al. (2014, 2012) and Ozer et al. (2009) detected changes in rainfall patterns in the region and connected them to changes in flood occurrence. Jury (2013) analyzed streamflow trends in Africa, including one station in the Niger basin (Niamey) and found an increase of streamflow that matched their general finding of a "return to wet conditions" in Africa in recent decades. Descroix et al. (2012, 2011) examined increasing river discharges in the Niger basin and came to the conclusion that adverse land-use change and crusting of soils lead to an increase in flooding as the climate in the region tends to become drier. For the Sahelian zone, this effect of increasing discharge despite decreasing rainfall is called the "Sahelian Paradox", first described by Albergel (1987). Sighomnou et al. (2013) attributed the extreme flooding of 2012 to the aforementioned changes in land use and crusting for the region around Niamey. Descroix et al. (2009) and Amogu et al. (2010) also addressed this phenomenon and found an increasing trend for streamflow of rivers in the Sahelian zone and a decreasing trend for rivers in the Sudanian zone. Descroix et al. (2013) summarized the results on the "Sahelian Paradox" and argued for a more regionalized assessment of the floods. Still, the role of climatic variability for the increased flood risk in the Niger basin has not been systematically addressed; neither has the associated damage been quantified.

Flood risk is not defined by flood frequency and magnitude alone, but by the product of value, vulnerability and hazards (Kron, 2005; Merz, 2006). Value in the formula is represented by the population that could be affected by floods in the basin. In West Africa, the population has multiplied ~ 2.5 times since 1980 (United Nations, Department of Economic and Social Affairs, 2013). For all countries in the Niger basin, the population growth rate is over 2 %, and for the Sahelian countries of Mali and Niger, even over 3 % (Central Intelligence Agency, 2013). The studies of Di Baldassarre et al. (2010) and Tschakert et al. (2010) provided evidence that the vulnerability of the population with regard to catastrophic floods has increased in the past due to several reasons, e.g. the loss of traditional knowledge about flood adaptation.

This study aims to contribute to the discussion with a comprehensive analysis of flooding and its damages in the Niger basin, thus attempting to disaggregate the total risk and attribute it to different flood risk components in the Niger basin. In order to take the regional heterogeneity of the Niger basin into account, we differentiate four subcatchments according to their main source areas and data availability (Guinean, Sahelian, Sudanian and Benue, Fig. 1).

We first evaluate the three most extensive databases on floods in Africa (NatCat database of Munich Re, Dartmouth Flood Observatory, International disaster database EM-DAT). The numbers of people affected are visualized spatially in order to see how the increase in people affected by floods during the past decades is associated with corresponding annual maximum discharges (AMAX) and rainfall in the subcatchments. In a second step, we focus on the timing of the AMAX and look for temporal shifts. Then, the time series are analyzed with regard to non-stationary trends and decadal patterns. Decadal patterns are correlated to the Atlantic Multidecadal Oscillation (AMO) in order to see whether this mode of variability can indicate flooding in the region.

Based on the systematic trend analysis, we use a data-based approach within a hypothesis-testing framework to attribute the detected trends (Merz et al., 2012). Therefore, rainfall data is analyzed and correlated to AMAX, and the flashiness of the discharge is examined in order to distinguish between the influence of climatic variability and land-use change effects. A focus on the special case of the "Sahelian Paradox" allows a qualitative estimation of the magnitude of influence of land-use change compared to climate change signals. The results are then discussed with a holistic view of the increasing flood risk, taking into account the hazards, vulnerability and population growth.

2 Niger basin

The Niger basin covers a total area of approximately 2 156 000 km^2, of which only $\sim$ 1 270 000 km^2 contribute to the river discharge (Fig. 1) (Ogilvie et al., 2010). The whole basin is spread over the territory of ten countries: Guinea, Côte d'Ivoire, Mali, Burkina Faso, Algeria, Benin, Niger, Chad, Cameroon and Nigeria (Zwarts et al., 2005). It extends over different agro-climatic and hydrographic regions with individual topographic and drainage characteristics. The Niger runoff regime is affected by different types of reoccurring floods, which result from the geographic locations and characteristics of their main source areas. The first one is the Guinean Flood, which originates from the headwaters of the Niger in the low-altitude plateaus called the Guinean highlands during the rainy season between July and November (Figs. 2 and 6, Descroix et al., 2012). From here, the Niger and Bani Rivers flow into the Inner Niger Delta (IND). This vast inland delta covers an area of $\sim$ 36 000 km^2 in central Mali and comprises lakes and floodplains that are regularly flooded with large annual variations. It influences the hydrological regime of the Niger significantly by flattening and slowing down the peak of the annual flood (Liersch et al., 2012; Zwarts, 2010).

Most of the inflow in the middle section of the Niger basin comes from the plateaus of the right-bank subbasins. The vast subbasins to the left reach up into the central Sahara but only contribute a minor amount of inflow, and local contributories are endorheic most of the time (Amogu et al., 2010). The annual peak during the rainy season (July–November) in the mid-section of the Niger downstream of the IND is called the "Red Flood" or "Sahelian Flood", the latter of which will be used in this study for the second subregion Figs. 2 and 6, Descroix et al., 2012). The third flood we define in this study is the "Sudanian Flood", which originates from the part of the basin downstream of the Sahelian zone and contributes to the gauge Yidere Bode in Nigeria, also reaching into the Sahelian climate zone. The fourth flood we focus on here is the flood of the Benue River, which flows into the Niger at the Nigerian city of Lokoja. Coming from a high-altitude plateau, it is the largest tributary in terms of discharge and outreaches

NHESSD
2, 5171–5212, 2014

the Niger by about a third at the confluence near Lokoja. This part of the Niger basin will henceforth be referred to as “Benue” (Fig. 2). Finally, the Niger disembogues into the Gulf of Guinea forming the Niger Delta, a flat region characterized by swamps and lagoons (Andersen et al., 2005). As no discharge data were available for the region between Yidere Bode and the confluence of the Benue, nor for the part after the confluence, these parts are not included in the analysis.

There are five major dams in the Niger basin which influence the discharge regime of the Niger and its tributaries (Table 1). In the Action Plan for the Niger Basin of the Niger Basin Authority (NBA), several scenarios with additional major dams are listed, such as Fomi in Guinea and Taoussa in Mali, for example (Niger Basin Authority, 2007). Currently, only the Kandadji dam in the Niger is actually under construction.

The population density in the Niger basin ranges from less than one person per km^2 in the deserted North to over 1000 in rural areas in Nigeria and Mali (Fig. 3) (Nelson, 2004). Of the four regions on which this study focuses, the Sudanian zone and the Benue are the most densely populated, with many regions containing over 100 persons per km^2. But also in the riverine areas along the Niger River, many regions in the Upper Niger basin and the middle section have similar population densities. The population growth rate in the countries of the Niger basin is extreme, ranging from 2 to 3.5 % with the highest increases in the Sahelian countries of Mali and Niger (Central Intelligence Agency, 2013).

3 Methodology

3.1 Data

3.1.1 Data on people affected by floods

Data on people affected by catastrophic flooding were derived from three different sources: the NatCatService of the Munich Reinsurance Company (MunichRe, 2013), the EM-disaster data base of the University of Leuven, Brussels (EM-DAT, 2013) and the Global Active Archive of Large Flood Events of the Darthmouth flood observatory (Brakenridge, 2013). All data are based on media reviews of the respective organization and the collection of data from official sources. The latter archive derives additional information from remote sensing data. Only the period from 1980 to 2012 is considered here, because all datasets provide input for this period. All three sources provide additional information on whether the flood was a flash or river/areal flood. However, the quality of the data for West Africa is low, as there is no systematic and uniform assessment of floods. Some reports are on the village level, others on the regional or even national level. Therefore, a distinction between people affected in the Sudanian and Sahelian zones was not possible because most reports grouped the number of people affected for both these regions together (Fig. 3). Since most of the reports come from the media, the numbers reported are not verifiable and differ often substantially between sources. Still, they are the best available source for damage data on catastrophic floods in West Africa. The data was analyzed equally, and so even if absolute numbers are uncertain, trends in the data are assumed to be reliable.

3.1.2 Discharge, precipitation and Atlantic Multidecadal Oscillation data

Observed river discharge at a daily resolution was provided by the Global Runoff Data Centre (Fekete et al., 1999) and the Niger Basin Authority. In stations where the flood peak originating from the Guinean flood occurred after 31 December, the value was attributed to the previous year. The annual maximum discharge (AMAX) value of a certain year was only used if it was the global change point of the annual hydrograph and if we could reasonably eliminate the possibility that any missing values might have been higher. At the Ansongo, Niamey and Malanville stations, peaks for the Guinean and the Sahelian/Sudanian floods occur. The Sahelian and Sudanian peaks are limited to August through October and do not occur every year. Therefore, the AMAX time series for the Sahelian and Sudanian floods at these gauging stations have gaps for years where a separate peak could not be distinguished.

NHESSD
2, 5171–5212, 2014

To analyze precipitation in the regions, we used reanalysis data from the WATCH Forcing data ERA 40 (WFD) (Weedon et al., 2011) for the period from 1960 until 2001 and the WATCH Forcing data ERA interim, which is processed similarly on the ERA 40 reanalysis data set for the period from 1979 until 2012 (WFDEI) (Dee et al., 2011). The precipitation parameter of both data sets is sampled on a 0.5×0.5 grid. For analysis of the means, only the months during the rainy season (June–November) within the different subregions have been included (Fig. 1). For the analysis of heavy precipitation, we derived the 95th percentile of the daily precipitation per year. Both parameters of the reanalysis time series of WFD and WFDEI have been validated with observed rainfall data from stations in all subregions (Bamako in Mali, Gao in Mali, Niamey in Niger, Maradi in Niger, Garoua in Cameroon, Fig. 1) (Fig. S1 in the Supplement). The reanalysis data was interpolated to the location of the stations, and it shows good performance with regard to annual and heavy precipitation.

The Atlantic Multidecadal Oscillation (AMO) is a mode of variability occurring in the northern Atlantic Ocean and is derived from sea surface temperatures (Dijkstra et al., 2006). It is closely connected to the rainfall in West Africa (Knight et al., 2006; Nicholson et al., 2000). The data on the AMO is provided by the National Oceanic and Atmospheric Administration (NOAA) in an unsmoothed version (Enfield et al., 2001) which is based on the Kaplan Extended Sea Surface Temperature dataset.

3.2 Statistics

3.2.1 Standard statistical methods

For the analysis of several time series, the local regression fitting technique LOESS was used (Cleveland and Devlin, 1988). It is a nonparametric regression method that combines multiple regression models in a k-nearest-neighbor-based meta-model. When plotted, it generates a smooth curve through a set of data points (LOESS Curve).

For correlation analysis, Spearman's rank correlation was applied. It is a nonparametric measure of the statistical dependence between two variables and is widely used to assess monotonic relationships between parameters.

Monotonic linear trends were identified using the Mann–Kendall test (Mann, 1945). This is a robust nonparametric test in which each element is compared with its successors and ranked as larger, equal or smaller. On this basis, it is possible to test the statistical significance of rejecting the null hypothesis (for all tests $\alpha = 0.05$). The linear trend was estimated using the Theil–Sen approach (Sen, 1968; Theil, 1950). Since serial independence is a requirement of the Mann–Kendall test, we checked beforehand for autocorrelations in all precipitation and hydrologic time series using the Durbin–Watson statistic test (Durbin and Watson, 1950, 1951). If an autocorrelation of the first order was found, trend-free pre-whitening was applied according to the method proposed by Yue et al. (2002): first, the trend estimated with the Theil–Sen approach was removed from the time series. Then, the first-order autocorrelation coefficient was calculated and subtracted from the time series. Finally, the trend was added back to the autocorrelation data and the Mann–Kendall test was applied in order to test for its significance.

In order to determine whether there was a trend influencing AMAX in addition to the trend in the rainfall amount, we detrended the AMAX and the precipitation time series for the corresponding rainy season in the region by subtracting the residuals of the linear trend. We then formulated the coefficient between these two time series analogous to the common runoff coefficient between mean discharge and precipitation (Fig. 7).

3.2.2 Changepoint identification

In order to detect changepoints in the means of datasets, the cumulative sums method (CUSUM) of Page (1954) is a common approach. Combined with an algorithm to minimize the cost function (Eq. 1) it is able to detect multiple changepoints (Killick et al., 2012):

$$\sum_{i=1}^{m+1} \left[C\left(Y\left(t_{i-1}+1\right):t_i\right)\right] + \beta f(m) \quad (1)$$

C is the cost function of the time series segment $Y(t_{i-1}+1):t_i$ and $\beta f(m)$ is the penalty function. Different algorithms exist to minimize this function, and for this study the Segmented Neighborhood (SN) method of Auger and Lawrence (1989) is appropriate because it is an exact approach and the datasets are relatively small so that the generally high computational cost of this method is acceptable. The cost functions for all possible segments are iteratively calculated. By that means, SN is able to compute the segments; however, it does not provide information about the number of segments which would be identical with the number of observations without restrictions. In order to prevent this overfitting, the penalty function was introduced. In this study, we used Akaike's Information Criterion (AIC) (Akaike, 1974)

$$\mathrm{AIC} = 2k - 2\ln(L) \quad (2)$$

where K is the number of parameters in the model and L is the maximized value of the likelihood function.

3.2.3 Wavelet analysis of annual maximum discharge time series

For detecting changes in the frequency of AMAX, we applied a wavelet power spectrum (Torrence and Compo, 1998). This can be described as a correlation coefficient between a dataset and a given function. This function slides over the dataset and is scaled to account for different frequencies. In our case we used the Morlet function, a complex nonorthogonal function which is commonly used for hydrographical time series (e.g. Delgado et al., 2010). The wavelet analysis is a powerful tool to show changes in the frequency over time, and indicates whether trends exist in the variance of the time series.

NHESSD
2, 5171–5212, 2014

3.2.4 Non-stationary Generalized Extreme value distribution

Non-stationary Generalized Extreme value models (NSGEV) (Coles et al., 2001) have been proven to be an effective tool not only to detect trends in the flood average but also of flood variability (e.g. Delgado et al., 2010; Hundecha et al., 2008). The method is described in detail by Delgado et al. (2010) and is based on the generalized extreme value function (GEV), which is cumulatively written as:

$$F(x) = \begin{cases} \exp\left[-\left(1-\frac{\xi}{\sigma}(x-\mu)\right)^{\frac{1}{\xi}}\right] & \text{if } \xi \neq 0 \\ \exp\left[-\exp\left(-\frac{x-\mu}{\sigma}\right)\right] & \text{if } \xi = 0 \end{cases} \tag{3}$$

with μ as the location parameter, σ as the scale parameter and ξ as the shape parameter. This cumulative distribution is then fitted systematically with different combinations of linear, second- and third-degree time-dependent parameters, however only for the location and shape parameters. These time-dependent parameters were then inserted in a maximum likelihood function.

$$L = \prod_{t=1}^{n} \sigma(t)^{-1} \exp\left[-\left(1-\xi\frac{x(t)-\mu(t)}{\sigma(t)}\right)\right] \tag{4}$$

Instead of the different parameters, the linear, second- or third-degree terms were inserted in the likelihood function. In order to identify the parameter setting which fits best to the data, a likelihood deviance statistic was applied. By this means, it could be tested whether the model of higher complexity from stationary to third-degree is an improvement, and whether this improvement is not just obtained by chance but is rather significant. So, each model M_1 was tested against the simpler model M_0. The deviance statistic of the models $\mathrm{M}_0 \subset \mathrm{M}_1$ is defined as

$$D = 2\left\{\ell_1(\mathrm{M}_1) - \ell_0(\mathrm{M}_0)\right\} \tag{5}$$

NHESSD
2, 5171–5212, 2014

where $\ell_1(M_1)$ and $\ell_0(M_0)$ are the maximized log-likelihoods for the models. The distribution D is asymptotic, and its degree of fit can be tested with a Chi-square test (χ^2_k). The degrees of freedom k express the difference in dimensionality between M_0 and M_1. So, larger values of D suggest that model M_1 explains the variation in the data better than M_0 and is therewith accepted as the NSGEV distribution.

3.2.5 Richards–Baker flashiness index

Changes in flashiness of the streamflows are quantified using the Richards–Baker Flashiness Index (Baker et al., 2004). This index F_{R-B} is based on the ratio of absolute day-to-day fluctuations in streamflow relative to the total flow in a year:

$$F_{R-B} = \frac{\sum_{i=1}^{n} |q_i - q_{i-1}|}{\sum_{i=1}^{n} q_i} \quad (6)$$

where q is the daily discharge of day i of the year (n = 365).

4 Results

4.1 Analysis of damage statistics

In Fig. 3, the number of people affected by catastrophic floods in the Niger basin per year for the period from 1980 to 2012 is displayed (note the algorithmic scale in the plot). The differences between the numbers for the three sources (see Sect 3.1.1) is small for most of the years, though for some years at least one source has strong underestimations, e.g. the NatCatService for 1988 or the Darthmouth Flood Observatory data for 2009 and 2011. The increase in flood frequency since the new millennium is striking. During the 1980s, around 120 000 were affected by catastrophic flooding according to the reports, over 500 000 in the 1990s, and well over 10 million from 2000 until 2012. In addition, the increase in people affected appears exponential when taking into account that the scale is logarithmic.

In Fig. 1, these floods are spatially plotted and flash floods were separated from areal and river floods, since both have different underlying mechanisms. The majority of the floods are river and areal floods and only a small proportion of the catastrophic floods are flash floods. Figure 1 also shows that floods in the Niger basin are relatively homogeneously distributed along the river and its tributaries, and that clustering is limited. The locations with the largest number of catastrophic floods between 1985 and 2012 have been reported along the main stem of the Niger River, e.g. around the cities of Bamako, Niamey, Maradi and in the upper Benue, while they have been less frequent in the Delta.

In Fig. 4, the numbers of people affected by floods are plotted in relation to the anomalies of the annual maximum discharge (AMAX) and the anomalies of the rainfall from reanalysis products (WFD, WFDEI) for each subregion. Changepoints were detected for the mean of the AMAX time series for each subregion. Since the Inner Niger Delta (IND) has a strong influence on the AMAX, stations within the reach of the wetland were excluded in the analysis for the Guinean region and only the stations upstream of the Delta (Kouroussa, Koulikoro and Douna) were considered. The Guinean region includes the gauges with the longest discharge observations and six changepoints were detected between 1910 and 2012. For the Sahelian and Sudanian regions, data is available starting in the 1950s and for both regions two changepoints were detected. For these three regions, there was a changepoint around 1970 and an additional one around 1990. For the Benue basin, data is only available from 1970 and only one changepoint at the beginning of the 1990s was detected. For the Guinean, Sudanian and Benue sub-basins, the last changepoint was detected in 1992, and for the Sahelian subregion the last changepoint was detected 5 years earlier in 1987. When all stations affected by the Guinean flood, including the IND, were taken into account, the latter two changepoints were not detected. This effect can be explained by retention processes in the wetland that smooth the hydrograph (Fig. S2 in the Supplement).

NHESSD
2, 5171–5212, 2014

The AMAX Loess curves of all regions show a decrease after 1970 that reaches its lowest point in the Guinean region after 1990 and in the other regions around 1980. For the Sahelian, Sudanian and Benue regions, the mean for the last period beginning around 1990 is approximately 25 % higher than the mean of the antecedent period beginning around 1970. In the Guinean region, the mean of the last period beginning here around 1970 is around 25 % lower than the antecedent period in the 1960s. In the Sahelian and Sudanian regions, this step is around −50 %.

The precipitation anomalies from 1960 to 2001 from the Watch Forcing Data (WFD) and from 1979 to 2012 from the Watch Forcing Data ERA Interim (WFDEI) show the same pattern in all regions. The mean decreases until the mid-1980s up to −10 % and again increases afterwards by around 10 %. The anomalies in the Sahelian region are the most distinct (more than ±30 %).

The number of people affected per year from 1985 to 2012 (see Sect. 3.1.1) are plotted at the bottom of each region. Note that it was not possible to distinguish between the Sudanian and Sahelian regions in the data sources, so the joint numbers are plotted for both of the regions (see Sect. 3.1.1). The scale is logarithmic, but a positive trend is nevertheless visible for the Sahelian, Sudanian and Benue regions. It is not visible for the Guinean region, but in all four regions there is a statistically significant linear trend when tested with the Mann–Kendall test. In addition, there is a strong correlation between AMAX and the number of people affected for the Sahelian, Sudanian and Benue regions (Spearman's ρ: 0.67, 0.63, 0.63). For the Guinean region, the correlation is weak at $\rho = 0.37$.

4.2 Analysis of changes in the timing of annual flood peaks

The occurrence of the flood peak as one day of the year was analyzed for all regions. A trend test starting in the year of the last changepoint could not reveal a significant linear trend for any of the time series (Guinean, Sudanian, Benue: 1992, Sahelian: 1987) (for example, see Fig. 5, left). This does not hold for the stations influenced by the dynamics of the Inner Niger Delta (IND) (Fig. 5, right). For these stations, significant trends exist which reflect the trends of the AMAX time series. This can be explained by the strong correlation between AMAX and the day of the year, caused by the basin effect of the IND. The water from the Guinean subregion accumulates in the IND and only a limited amount can pass through the outlet near Diré. Accordingly, the delay in AMAX at the affected downstream stations is dependent on the total amount of water in the Delta. Due to this correlation, the positive trend in AMAX causes a significant change in the timing of the AMAX of the Guinean Flood in and downstream of the IND.

4.3 Trend analysis of annual flood peaks

In Fig. 6, the AMAX time series are analyzed using non-stationary generalized extreme value functions (NSGEV). Since an analysis of the mean for all stations in one subregion might balance out changes in the frequency, the most complete time series for each subregion has been selected for the trend detection. For the Guinean region, Kouroussa was selected because the flow is not influenced by the IND. For the Benue region, no time series was long enough for the analysis. In order to avoid the complex distributions of the whole time series that change their directions several times, the analysis was limited to the period after the changepoint around 1970 which was identified by the changepoint analysis in all regions. For the Guinean region, a model with a constant shape parameter but a third-degree location parameter was most suitable for explaining the distribution of probabilities for the AMAX time series. The curve changed from higher discharge ($\sim 1200\,m^3\,s^{-1}$) in 1969 to lower ($\sim 500\,m^3\,s^{-1}$) discharges in the 1970s and 1980s, and then half-way back up ($\sim 800\,m^3\,s^{-1}$) by 2012. For the Sahelian and Sudanian time series models, a linear trend in the location parameter and again a constant shape parameter show the best fit. In the Sahelian region, the peak moved from ~ 750 to $1500\,m^3\,s^{-1}$ and in the Sudanian region from ~ 1200 to $1700\,m^3\,s^{-1}$. In the Sudanian and Sahelian regions together, the distributions are flatter than in the Guinean region. This means that the frequency of the AMAX in the analyzed subregions do change linearly, meaning that an exemplary increase in the mean annual flood peak of $100\,m^3\,s^{-1}$ would result in a corresponding increase for the

50 or 500 year return interval of 100 $m^3 s^{-1}$, as well. The analysis suggests that linear models are sufficiently complex to explain the dynamics of AMAX during the period analyzed, from the beginning of the dry conditions around 1970 until 2012. In addition, the linear trends found confirm the positive trends observed in AMAX (Sect. 4.1) for the Sahelian and Sudanian time series since the 1970s and for the Guinean time series since the 1980s.

In order to verify the results of the NSGEV, wavelet power spectra are applied to the same time series (Fig. S3 in the Supplement) none of the wavelets could a significant change in variance be detected during the last four decades, which supports the finding that no changes in variability occurred in AMAX, but only linear trends for the flood magnitude.

4.4 Attribution of changes in annual flood peaks

4.4.1 Analysis of precipitation, heavy precipitation, runoff coefficients and flashiness

Figure 7 presents the AMAX, the annual precipitation in the corresponding hydrological year and, as a measurement for heavy precipitation, the 95th percentile of the daily precipitation for the four subregions. Since the NSGEV distribution of the subregions revealed linear models to be best suitable after 1980, we limited the analysis to this time period. In addition, this timespan also corresponds to the period when the data on people affected by floods was available.

We found a significant positive trend for the AMAX, annual precipitation and heavy precipitation in all four regions. The test for autocorrelation was only positive for the AMAX time series of the Guinean region. Here, we then removed the autocorrelation as described in Sect. 3.2.1. The strongest trend for AMAX with an increase between 30 and 40 % can be found in the Sahelian, Sudanian and Benue regions. In the Guinean region, the trend for AMAX is ~ 20 % until 2012. The annual precipitation during the same period increased ~ 15 % in the Guinean, Sahelian and Sudanian regions, and only ~ 10 % in the Benue region. The heavy precipitation expressed by the 95th percentile increased proportionally in all regions between 20 and 30 %.

The coefficient between the detrended AMAX and the detrended precipitation time series in the corresponding rainy season did not show a significant trend in any of the regions. We also tested trends for the runoff coefficient with the detrended time series of the mean discharge and the rainfall in the rainy season. It showed the same temporal characteristics, and the curve was very similar to the coefficient for AMAX and contained neither trend (not shown).

Figure 8 shows the anomaly of flashiness via the yearly Richards–Baker index for discharge data and heavy precipitation as the 95th percentile for the four subregions. For Koulikoro and Niamey, there are significant positive trends in flashiness since 1960, which increase greater than heavy precipitation. Especially for the Sahelian gauge Niamey, this increase is extreme, from ~ −50 to ~ +40 %. For Malanville in the Sudanian region, the gaps in the daily data are too large to estimate a trend in the flashiness. Still, the available data also indicates an increase in flashiness. In contrast, the gauge at Lokoja indicates a minor decrease in flashiness after the millennium.

4.4.2 Correlations with the Atlantic Multidecadal Oscillation

In order to determine whether the Atlantic Multidecadal Oscillation (AMO) could provide information on flood magnitudes and trends, the similarity of patterns and correlations were evaluated. The changepoints in the AMO were identified for the same period for which discharge data is available (1907–2012) (Fig. 9). The three changepoints found for the AMO correspond to points found for the AMAX time series. The point in the beginning of the twenties is reflected in the changepoint in the Guinean AMAX and the changepoint at the beginning of the 1990s in the Benue, Sudanian and Guinean regions upstream of the IND. However, the changepoint detected for the AMO at the beginning of the 1960s is delayed in the AMAX time series of all regions around 1970. The correlation between the AMO and AMAX is moderate for all regions and has a ρ of around 0.5 (Table 2, Fig. S4 in the Supplement). The correlation of the AMO with the

NHESSD
2, 5171–5212, 2014

precipitation is also moderate in the respective source regions. In the Guinean region, the value is higher compared to the AMAX, with $\rho = 0.54$. For the other regions, ρ is slightly smaller (around 0.45, see Table 2).

4.4.3 The "Sahel Paradox"

The flood originating in the Guinean highlands experiences its peak before it enters the IND, usually around October. Due to the increasing distance and the buffering/retention effect of the wetlands, the flood peak leaves the IND with a delay of approximately three months. Therefore, it arrives in the middle section of the Niger around Jan although rainfall in the Sahelian region falls at the same time as in the Guinean highlands. Thus, here the Guinean and Sahelian regimes generate a flood which can usually be clearly distinguished (exemplarily shown for the Niger at Niamey in Fig. 10). The peak of the Guinean flood is already smoothed due to the large watershed and by the dynamics of the IND, whereas the peak of the local Sahelian flood is more jagged and separated into different peaks for local tributaries (Descroix et al., 2012).

In Fig. 11, the evolution of AMAX for both flood peaks at Niamey is plotted in relation to the annual precipitation in the corresponding source area. For the Sahelian peak, heavy precipitation is also plotted. For the Guinean peak, heavy precipitation is not shown, since the source area in the Guinean highlands is located ~ 1500 km from the gauge in Niamey and these events do not have a noticeable effect here. The systematic detection of the Sahelian peak supports the finding of Descroix et al. (2012) that the AMAX regime in the middle section of the Niger has changed distinctively over the past 30 years. Between 1930 and 1980, a year with a separate peak for the Sahelian flood was rather an exception in Niamey (see also the differences in Fig. 10). Since 1983, only one year showed no separate Sahelian peak and since then, the peak was even higher for nine years compared to the Guinean flood (Fig. 11, top). This effect is connected to the "Sahelian Paradox", which is illustrated in Fig. 11 for the Sahelian peak. The positive trend in AMAX of the Sahelian peak already started in the 1970s. In contrast, the related rainfall data shows a further decrease in annual precipitation until

NHESSD
2, 5171–5212, 2014

the middle of the 1980s. The data for heavy precipitation in the region shows similar trends and turning points as that for annual precipitation. Therefore, heavy precipitation cannot explain the paradox of increasing discharge despite decreasing rainfall. Since the end of the 1980s, all three trends show the same direction and hence the paradox does not exist anymore, even if the underlying process might still be continuing. For the Guinean peak, this effect is completely absent and the evolution of the AMAX series corresponds to the annual precipitation. For the time series of the Guinean flood peak, the minimum for AMAX and precipitation are located in the middle of the 1980s, i.e. analogues to the precipitation in the Sahelian region. Hence, the Sahelian and Guinean flood peaks are decoupled even when observed at the same gauging station.

5 Discussion

5.1 The return to wet conditions and the increasing number of catastrophic floods

The concurrence of changepoints for the annual maximum discharge (AMAX) time series in the regions with a changepoint around 1970 and another around 1990 (Fig. 4) supports the findings by previous studies of a decadal climatic pattern in West Africa (e.g. Nicholson et al., 2000; Sarr et al., 2013). The period from ~ 1970 to ~ 1990 was in general exceptionally dry in West Africa, and this also holds for the flood peaks. In the Sahelian, Sudanian and Benue regions, the mean during this period was ~ 35 % lower compared to the preceding period. The subsequent return of wetter conditions in West Africa (Jury, 2013) is again reflected in increased flood peaks which almost reach the same level as before the dry period. In the Guinean region, the recovery is less distinct and the flood peaks started to increase again later. In all regions, the positive trend is continuing (Fig. 7). Especially in the Sahelian region, the AMAX reached levels in recent years that have not been observed since recording began (Fig. 11). Particularly remarkable is the increase in frequency and magnitude of Sahelian flooding, which

NHESSD
2, 5171–5212, 2014

was also found by Descroix et al. (2012). Even in the wet 1960s, the Guinean flood peak was always higher than the Sahelian peak. This changed during the last three decades, and the trend for the Guinean and Sahelian floods are now decoupled. Since 1980, the Sahelian flood was higher than the Guinean in nine of the years. In Niamey, the flood peak of 2012 was the highest peak since the beginning of records in 1929 (Fig. 11, top). Further downstream in the Sudanian region, we see the same decoupled patterns; however, the trend is less distinct and the AMAX does not reach the values of the 1960s (Fig. 8, bottom).

The increasing AMAX in all four regions is not connected to a change in the flood regime. The distribution of the extreme stays the same, but on a different level (Fig. 6). Especially in the case of the Kouroussa gauge in the Guinean region, we can see that the shape of the distribution moved from the higher level at the beginning of the 1970s to a lower level, and stabilized in the recent past to a level between the two latter stages. This holds also for the Sahelian and Sudanian regions; however, the change in the location parameter is more distinct for the Sahelian station Niamey.

The patterns of increasing AMAX magnitudes are reflected by the number of people affected by floods in all the regions (Fig. 3). The trend is significant as well, and strongly correlated to the AMAX in all regions (Fig. 4). The most extreme increase, an exponential increase, occurs in the Sahelian and Sudanian regions. In Fig. 1, we can see no difference in the number of catastrophic floods reported for the four regions. The marks are distributed along the Niger River and its tributaries without showing a distinct cluster in the Sahelian and Sudanian regions. However, the number of people affected shows distinct differences in the recent past for these two regions when compared to the other parts of the basin. We explain the more extreme increase in people affected by floods for the Sudanian and Sahelian regions with two main causes. First, the increase in the level of AMAX compared to the preceding periods is more pronounced than in the other regions (see Sect. 5.2). In the Guinean and Benue regions, flood plains such as the IND or the Benue wetlands (Uluocha and Okeke, 2004) are inundated in case of a flood event and thereby reduce high flood peaks, while in the drier regions these retention areas are missing, leading to higher flood peaks and subsequently more "catastrophic" events in these areas. Second, the population increase in these subregions is about 1 % greater compared to the more southern subregions (Central Intelligence Agency, 2013). In addition, in these regions the traditional knowledge of strategies for handling flood magnitudes might be less widespread than in wetter subregions (Tschakert et al., 2010). In the Guinean and Benue regions some of the traditional knowledge might still exist, since in these regions the current flood levels are still lower than those experienced during the 1960s.

5.2 Attribution of the changes in the flood regime and the "Sahelian paradox"

The evolution of AMAX in the Niger basin is closely related to the evolution of the Atlantic Multidecadal Oscillation (AMO) (Fig. 9). The correlations between the AMO and the AMAX, as well as for the precipitation, are high for all subregions. The dry periods around the 1970s and 1980s (Fig. 4) reflect the negative values of the AMO, and the recovery occurring since the 1990s can be also explained by its changes. The extremely high AMO values in the years 1998 and 2012 resulted in major flooding events in the same years in the Niger basin, with exceptional high AMAX values (Fig. 4).

The question of whether climatic variabilities or land-use changes are the dominant drivers of the increasing AMAX is complex. The focus on the "Sahelian Paradox" reveals most clearly the influence of both drivers. The extreme increase in flashiness for Niamey after 1960 supports the influence of land-use change (Fig. 8). Sealed soils, crusting and deforestation lead to more direct runoff due to less infiltration, as proposed by Descroix et al. (2012). Figure 11 illustrates the fact that the increase in heavy precipitation started later than the increase in AMAX. Therefore, heavy precipitation can be excluded as the cause of the "Sahelian Paradox"; instead, land-use change is the most plausible explanation.

Descroix et al. (2012) concluded that, based on their findings of decreasing rainfall, the recent increase in flooding in the Sahelian region and especially in the region around Niamey are not related to a climatic changes but only to land cover changes due to more intensive agricultural use. However, our findings contradict this conclusion for the Sahelian region and the other subregions. The trend prevailing since the 1990s in rainfall as well as in extreme events is significant and can at least partly explain the increase in AMAX. In addition, the absence of a trend in the detrended runoff coefficient time series indicates that land-use change at least plays no dominant role in the increase in AMAX (Fig. 7). The increase in precipitation as the driver for the increased flooding in the Sahelian region is a fact also supported by Aich et al. (2014). The study shows that for four basins in Africa an increase in precipitation in drier regions with a rather low runoff coefficient leads to proportionally higher increases in discharge compared to regions with a wetter climate, where an increase in precipitation has less influence. Hence, wet years in the dry Sahelian and, less distinctly, in the Sudanian region, lead to proportionally higher discharges than in the Guinean or Benue regions of the Niger basin.

Also, the non-linear trend in heavy precipitation (Fig. 7) supports the view that climatic variability is the main driver of the change. The study by Panthou et al. (2014) comes to the same results by analyzing a multitude of rainfall stations in the Sahel region with up-to-date statistical methods. They were also able to detect a significant trend of extreme events increasing. These results contradict the findings of Descroix et al. (2012) for the Sahelian region, who detected trends neither for total precipitation nor for heavy precipitation. In their study, they analyzed station data from one weather station at Niamey collectively for 5 decades from 1960 to 2010. However, there is a significant trend in the observed data for Niamey for the period 1980–2013 in the annual precipitation and an even stronger trend in the heavy precipitation (Fig. S1 in the Supplement) both of which correspond to the trends detected in the reanalysis data.

6 Conclusions and summary

The increasing flood risk in the Niger basin is caused by an increase in all three relevant factors: population, vulnerability and hazards. The substantial increase in inhabitants affected by floods in the Sahelian and Sudanian subregions is the result of the greatest increase in all of these factors in these subregions. With regard to the hazards, we find evidence for a general return to wet conditions since the end of the 1980s in time series of annual maximum discharge (AMAX) and precipitation in the Niger basin. The Non-stationary Generalized Extreme value (NSGEV) and wavelet analysis show linear trends in AMAX. No change in the variance and form of distribution occurred in the last three decades. The Atlantic Multidecadal Oscillation is strongly correlated to the AMAX, and might be worth considering for use as an indicator of flood risk, e.g. for dam management.

With regard to the causes of the increased flood hazards and the AMAX, we identified the variability and trends in precipitation in the Niger basin as the main causes. The changes in flashiness prove the influence of land-use change on the hydrograph; however, the analysis of changes in the runoff coefficient reveals that this effect does not determine the magnitude of AMAX. In the special case of the "Sahel Paradox", the effect of land-use change on the magnitude of AMAX becomes visible, but also here precipitation seems to play the major role in the increase. In order to quantify the share of annual precipitation, land-use change, and the non-linear increase in heavy precipitation, a detailed modelling study could bring more clarity and provide conclusive evidence. In addition, the role of groundwater in the region is very complex (Leduc et al., 2001; Mahé, 2009) and should be addressed systematically. Detailed modelling studies on a subregional level are also necessary to project future flood risks in the Niger basin. Such an effort should include land-use change and population vulnerability. In order to halt the trend of increasing flood risk, especially in the Sahelian and Sudanian subregions, the action plan of the NBA should be implemented, which includes more dams. In addition, more adapted settlement and housing policies are required and early warning systems based on forecasting and hydrological modelling should be implemented in the Niger basin.

The Supplement related to this article is available online at doi:10.5194/nhessd-2-5171-2014-supplement.

Acknowledgements. We thank the IMPACT2C project for financing this study and the Niger Basin Authority (NBA) for providing data.

References

Aich, V., Liersch, S., Vetter, T., Huang, S., Tecklenburg, J., Hoffmann, P., Koch, H., Fournet, S., Krysanova, V., Müller, E. N., and Hattermann, F. F.: Comparing impacts of climate change on streamflow in four large African river basins, Hydrol. Earth Syst. Sci., 18, 1305–1321, doi:10.5194/hess-18-1305-2014, 2014.

Akaike, H.: A new look at the statistical model identification, IEEE T. Automat. Contr., 19, 716–723, doi:10.1109/TAC.1974.1100705, 1974.

Albergel, J.: Sécheresse, désertification et ressources en eau de surface. Application aux petits bassins du Burkina Faso, in: The Influence of Climate Change and Climatic Variability on the Hydrologie Regime and Water Resources, Proceedings of the Vancouver Symposium, 9-22 August 1987, IAHS Publication Vol. 168, 355–445, available from: http://itia.ntua.gr/hsj/redbooks/168/hysj_168_01_0355.pdf (last access: 6 February 2014), 1987 (in French).

Amogu, O., Descroix, L., and Yéro, K.: Increasing river flows in the Sahel?, Water, available at: http://www.mdpi.com/2073-4441/2/2/170 (last access: 11 November 2013), 2010.

Andersen, I., Dione, O., Jarosewich-Holder, M., and Olivry, J. C.: Niger River Basin: A Vision for Sustainable Management (Directions in Development), edited by: Golitzen, K. G., World Bank Publications, Washington DC, available at: http://www.amazon.com/Niger-River-Basin-Sustainable-Development/dp/0821362038 (last access: 11 November 2013), 2005.

Auger, I. and Lawrence, C.: Algorithms for the optimal identification of segment neighborhoods, B. Math. Biol., 51, 39–54, doi:10.1016/S0092-8240(89)80047-3, 1989.

Baker, D. B., Richards, R. P., Loftus, T. T., and Kramer, J. W.: A new flashiness index: characteristics and applications to midwestern rivers and streams, J. Am. Water Resour. As., 40, 503–522, doi:10.1111/j.1752-1688.2004.tb01046.x, 2004.

Brakenridge, G. R.: Global Active Archive of Large Flood Events, available at: http://floodobservatory.colorado.edu/Archives/index.html (last access: 12 August 2014), 2013.
Central Intelligence Agency: The World Factbook 2013-14, available at: https://www.cia.gov/library/publications/the-world-factbook/index.html (last access: 12 August 2014), 2013.
Cleveland, W. S. and Devlin, S. J.: Locally weighted regression: an approach to regression analysis by local fitting, J. Am. Stat. Assoc., 83, 596–610, doi:10.1080/01621459.1988.10478639, 1988.
Coles, S., Bawa, J., Trenner, L., and Dorazio, P.: An Introduction to Statistical Modeling of Extreme Values, Springer London, London, UK, 2001.
Dee, D. P., Uppala, S. M., Simmons, A. J., Berrisford, P., Poli, P., Kobayashi, S., Andrae, U., Balmaseda, M. A., Balsamo, G., Bauer, P., Bechtold, P., Beljaars, A. C. M., van de Berg, L., Bidlot, J., Bormann, N., Delsol, C., Dragani, R., Fuentes, M., Geer, A. J., Haimberger, L., Healy, S. B., Hersbach, H., Hólm, E. V., Isaksen, L., Kållberg, P., Köhler, M., Matricardi, M., McNally, A. P., Monge-Sanz, B. M., Morcrette, J.-J., Park, B.-K., Peubey, C., de Rosnay, P., Tavolato, C., Thépaut, J.-N., and Vitart, F.: The ERA-Interim reanalysis: configuration and performance of the data assimilation system, Q. J. Roy. Meteor. Soc., 137, 553–597, doi:10.1002/qj.828, 2011.
Delgado, J. M., Apel, H., and Merz, B.: Flood trends and variability in the Mekong river, Hydrol. Earth Syst. Sci., 14, 407–418, doi:10.5194/hess-14-407-2010, 2010.
Descroix, L., Mahé, G., Lebel, T., Favreau, G., Galle, S., Gautier, E., Olivry, J.-C., Albergel, J., Amogu, O., Cappelaere, B., Dessouassi, R., Diedhiou, A., Le Breton, E., Mamadou, I., and Sighomnou, D.: Spatio-temporal variability of hydrological regimes around the boundaries between Sahelian and Sudanian areas of West Africa: a synthesis, J. Hydrol., 375, 90–102, doi:10.1016/j.jhydrol.2008.12.012, 2009.
Descroix, L., Esteves, M., Souley Yéro, K., Rajot, J.-L., Malam Abdou, M., Boubkraoui, S., Lapetite, J. M., Dessay, N., Zin, I., Amogu, O., Bachir, A., Bouzou Moussa, I., Le Breton, E., and Mamadou, I.: Runoff evolution according to land use change in a small Sahelian catchment, Hydrol. Earth Syst. Sci. Discuss., 8, 1569–1607, doi:10.5194/hessd-8-1569-2011, 2011.
Descroix, L., Genthon, P., Amogu, O., Rajot, J.-L., Sighomnou, D., and Vauclin, M.: Change in Sahelian Rivers hydrograph: the case of recent red floods of the Niger River in the Niamey region, Global Planet. Change, 98–99, 18–30, doi:10.1016/j.gloplacha.2012.07.009, 2012.

NHESSD
2, 5171–5212, 2014

Descroix, L., Bouzou, I., Genthon, P., Sighomnou, D., Mahe, G., Mamadou, I., Vandervaere, J.-P., Gautier, E., Faran, O., Rajot, J.-L., Malam, M., Dessay, N., Ingatan, A., Noma, I., Souley, K., Karambiri, H., Fensholt, R., Albergel, J., and Olivry, J.-C.: Impact of drought and land – use changes on surface – water quality and quantity: the Sahelian paradox, in: Current Perspectives in Contaminant Hydrology and Water Resources Sustainability, edited by: Bradley, P., 243–271, InTech, Rijeka, Croatia, 2013.

Di Baldassarre, G., Montanari, A., Lins, H., Koutsoyiannis, D., Brandimarte, L., and Blöschl, G.: Flood fatalities in Africa: from diagnosis to mitigation, Geophys. Res. Lett., 37, L22402, doi:10.1029/2010GL045467, 2010.

Dijkstra, H. A., Raa, L., Schmeits, M., and Gerrits, J.: On the physics of the Atlantic Multidecadal Oscillation, Ocean Dynam., 56, 36–50, doi:10.1007/s10236-005-0043-0, 2006.

Durbin, J. and Watson, G.: Testing for serial correlation in least squares regression. I, Biometrika, 37, 409–428, available at: http://biomet.oxfordjournals.org/content/37/3-4/409.short (last access: 10 March 2014), 1950.

Durbin, J. and Watson, G.: Testing for serial correlation in least squares regression. II, Biometrika, 38, 159–178, available at: http://www.jstor.org/stable/2332325 (last access: 10 March 2014), 1951.

EM-DAT: The OFDA/CRED International Disaster Database, Univ. Cathol. Louvain, Brussels, Belgium, available at: www.emdat.be (last access: 12 August 2014), 2013.

Enfield, D. B., Mestas-Nuñez, A. M., and Trimble, P. J.: The Atlantic Multidecadal Oscillation and its relation to rainfall and river flows in the continental US, Geophys. Res. Lett., 28, 2077–2080, doi:10.1029/2000GL012745, 2001.

Fekete, B. M., Vorosmarty, C. J., and Grabs, W.: Global, Composite Runoff Fields Based on Observed River Discharge and Simulated Water Balances, Federal Institute of Hydrology (BfG), Koblenz, Germany, 1999.

Hundecha, Y., St-Hilaire, A., Ouarda, T. B. M. J., El Adlouni, S., and Gachon, P.: A non-stationary extreme value analysis for the assessment of changes in extreme annual wind speed over the Gulf of St. Lawrence, Canada, J. Appl. Meteorol. Climatol., 47, 2745–2759, doi:10.1175/2008JAMC1665.1, 2008.

Jury, M. R.: A return to wet conditions over Africa: 1995–2010, Theor. Appl. Climatol., 111, 471–481, doi:10.1007/s00704-012-0677-z, 2013.

Killick, R., Fearnhead, P., and Eckley, I. A.: Optimal detection of changepoints with a linear computational cost, J. Am. Stat. Assoc., 107, 1590–1598, doi:10.1080/01621459.2012.737745, 2012.
Knight, J. R., Folland, C. K., and Scaife, A. A.: Climate impacts of the Atlantic Multidecadal Oscillation, Geophys. Res. Lett., 33, L17706, doi:10.1029/2006GL026242, 2006.
Kron, W.: Flood risk = hazard values vulnerability, Water Int., 30, 58–68, doi:10.1080/02508060508691837, 2005.
Leduc, C., Favreau, G., and Schroeter, P.: Long-term rise in a Sahelian water-table: the Continental Terminal in South-West Niger, J. Hydrol., 243, 43–54, doi:10.1016/S0022-1694(00)00403-0, 2001.
Liersch, S., Cools, J., Kone, B., Koch, H., Diallo, M., Reinhardt, J., Fournet, S., Aich, V., and Hattermann, F. F.: Vulnerability of rice production in the Inner Niger Delta to water resources management under climate variability and change, Environ. Sci. Policy, 34, 8–33, doi:10.1016/j.envsci.2012.10.014, 2012.
Mahe, G.: Surface/groundwater interactions in the Bani and Nakambe rivers, tributaries of the Niger and Volta basins, West Africa, Hydrol. Sci. J., 54, 704–712, doi:10.1623/hysj.54.4.704, 2009.
Mahe, G., Lienou, G., Descroix, L., Bamba, F., Paturel, J. E., Laraque, A., Meddi, M., Habaieb, H., Adeaga, O., Dieulin, C., Chahnez Kotti, F., and Khomsi, K.: The rivers of Africa: witness of climate change and human impact on the environment, Hydrol. Process., 27, 2105–2114, doi:10.1002/hyp.9813, 2013.
Mann, H. B.: Nonparametric tests against trend, Econometrica, 13, 245–259, 1945.
Merz, B.: Hochwasserrisiken: Möglichkeiten und Grenzen der Risikoabschätzung, E. Schweizerbartsche Verlagsbuchhandlung, Stuttgart, 2006 (in German).
Merz, B., Vorogushyn, S., Uhlemann, S., Delgado, J., and Hundecha, Y.: HESS Opinions “More efforts and scientific rigour are needed to attribute trends in flood time series”, Hydrol. Earth Syst. Sci., 16, 1379–1387, doi:10.5194/hess-16-1379-2012, 2012.
MunichRe: NatCatSERVICE, available at: http://www.munichre.com/en/reinsurance/business/non-life/georisks/natcatservice/default.aspx (last access: 6 February 2014), 2013.
Nelson, A.: African Population Database, UNEP GRID, Sioux Falls, 2004.
Nicholson, S. E., Some, B., and Kone, B.: An Analysis of Recent Rainfall Conditions in West Africa, Including the Rainy Seasons of the 1997 El Niño and the 1998 La Niñ a Years, J. Climate, 13, 2628–2640, doi:10.1175/1520-0442(2000)013<2628:AAORRC>2.0.CO;2, 2000.

NHESSD
2, 5171–5212, 2014

Niger Basin Authority, (NBA): Elaboration of an Action Plan for the Sustainalble Development of the Niger Basin. Phase 2: Master Plan for the Development and Managment, Niamey, Niger, 2007.

Ogilvie, A., Mahé, G., Ward, J., Serpantié, G., Lemoalle, J., Morand, P., Barbier, B., Diop, A. T., Caron, A., Namarra, R., Kaczan, D., Lukasiewicz, A., Paturel, J.-E., Liénou, G., and Clanet, J. C.: Water, agriculture and poverty in the Niger River basin, Water Int., 35, 594–622, available at: http://www.tandfonline.com/doi/abs/10.1080/02508060.2010.515545 (last access: 11 November 2013), 2010.

Ozer, P., Hountondji, Y., and Manzo, O. L.: Evolution des caractéristiques pluviométriques dans l'est du Niger de 1940 a 2007, Geo-Eco-Trop., 33, 11–30, available at: http://orbi.ulg.ac.be/handle/2268/78267 (last access: 6 February 2014), 2009.

Paeth, H., Fink, A. H., Pohle, S., Keis, F., Mächel, H., and Samimi, C.: Meteorological characteristics and potential causes of the 2007 flood in sub-Saharan Africa, Int. J. Climatol., 31, 1908–1926, doi:10.1002/joc.2199, 2011.

Page, E.: Continuous inspection schemes, Biometrika, 41, 100–114, available at: http://www.jstor.org/stable/2333009 (last access: 2 March 2014), 1954.

Panthou, G., Vischel, T., Lebel, T., Blanchet, J., Quantin, G., and Ali, A.: Extreme rainfall in West Africa: a regional modeling, Water Resour. Res., 48, W08501, doi:10.1029/2012WR012052, 2012.

Panthou, G., Vischel, T., and Lebel, T.: Recent trends in the regime of extreme rainfall in the Central Sahel, Int. J. Climatol., doi:10.1002/joc.3984, online first, 2014.

Sarr, M. A., Zoromé, M., Seidou, O., Bryant, C. R., and Gachon, P.: Recent trends in selected extreme precipitation indices in Senegal – a changepoint approach, J. Hydrol., 505, 326–334, doi:10.1016/j.jhydrol.2013.09.032, 2013.

Sen, P.: Estimates of the regression coefficient based on Kendall's tau, J. Am. Stat. Assoc., 63, 1379–1389, available at: http://amstat.tandfonline.com/doi/abs/10.1080/01621459.1968.10480934 (last access: 10 March 2014), 1968.

Sighomnou, D., Descroix, L., Genthon, P., Mahé, G., Moussa, I. B., Gautier, E., Mamadou, I., Vandervaere, J.-P., Bachir, T., Coulibaly, B., Rajot, J.-L., Issa, O. M., Abdou, M. M., Dessay, N., Delaitre, E., Maiga, O. F., Diedhiou, A., Panthou, G., Vischel, T., Yacouba, H., Karambiri, H., Paturel, J.-E., Diello, P., Mougin, E., Kergoat, L., and Hiernaux, P.: La crue de 2012 à Niamey?: un paroxysme du paradoxe du Sahel?, Sci. Chang. planétaires/Sécheresse, 24, 3–13, doi:10.1684/sec.2013.0370, 2013 (in French).

Tarhule, A.: Damaging rainfall and flooding: the other Sahel hazards, Climatic Change, 72, 355–377, doi:10.1007/s10584-005-6792-4, 2005.

Theil, H.: A rank-invariant method of linear and polynomial regression analysis, Ned. Acad. Wetensch. Proc., 53, 386–392, available at: http://link.springer.com/chapter/10.1007/978-94-011-2546-8_20 (last access: 10 March 2014), 1950.

Torrence, C. and Compo, G. P.: A practical guide to wavelet analysis, B. Am. Meteorol. Soc., 79, 61–78, doi:10.1175/1520-0477(1998)079<0061:APGTWA>2.0.CO;2, 1998.

Tschakert, P., Sagoe, R., Ofori-Darko, G., and Codjoe, S. N.: Floods in the Sahel: an analysis of anomalies, memory, and anticipatory learning, Climatic Change, 103, 471–502, doi:10.1007/s10584-009-9776-y, 2010.

Uluocha, N. O. and Okeke, I. C.: Implications of wetlands degradation for water resources management: lessons from Nigeria, GeoJournal, 61, 151–154, doi:10.1007/s10708-004-2868-3, 2004.

United Nations, Department of Economic and Social Affairs, P. D.: World Population Prospects: The 2012 Revision, Key Findings and Advance Tables, Working Paper No. ESA/P/WP.227, New York, 2013.

Weedon, G. P., Gomes, S., Viterbo, P., Shuttleworth, W. J., Blyth, E., Österle, H., Adam, J. C., Bellouin, N., Boucher, O., and Best, M.: Creation of the WATCH forcing data and its use to assess global and regional reference crop evaporation over land during the twentieth century, J. Hydrometeorol., 12, 823–848, doi:10.1175/2011JHM1369.1, 2011.

Yue, S., Pilon, P., Phinney, B., and Cavadias, G.: The influence of autocorrelation on the ability to detect trend in hydrological series, Hydrol. Process., 16, 1807–1829, doi:10.1002/hyp.1095, 2002.

Zwarts, L.: Will the inner Niger delta shrivel up due to climate change and water use upstream. A & W report 1537, Feanwâlden, available at: http://www.wetlands.org/Portals/0/publications/Report/WilltheInnerNigerDeltashrivelupduetoclimatechangeandwateruseupstream.pdf (last access: 11 November 2013), 2010.

Zwarts, L., Beukering, P. Van, Kone, B., and Wymenga, E.: The Niger, a Lifeline: Effective Water Management in the Upper Niger Basin, Altenburg & Wymenga Ecologisch Onderzoek BV, Leylstad, Netherlands, 2005.

Table 1. Major reservoirs in the Niger basin.

Reservoir	Country/River	Completion date	Max. volume [million m^3]*
Kainji	Nigeria/Niger River	1968	15 000
Selingué	Mali/Sankarani River	1982	2135
Lagdo	Cameroon/Benue River	1982	7800
Jeeba	Nigeria/Niger River	1984	3880
Shiroro	Nigeria/Kaduna River	1990	7000

* Including dead storage.

NHESSD
2, 5171–5212, 2014

Table 2. Spearman's correlations of the Atlantic Multidecadal Oscillation with AMAX and precipitation for the regions. All correlations are significant.

	Guinean	Sahelian	Sudanian	Benue
Corr (AMAX, AMO)	0.47	0.51	0.55	0.48
Corr (Prec., AMO)	0.54	0.46	0.45	0.45

NHESSD
2, 5171–5212, 2014

Floods in the Niger basin – analysis and attribution

V. Aich et al.

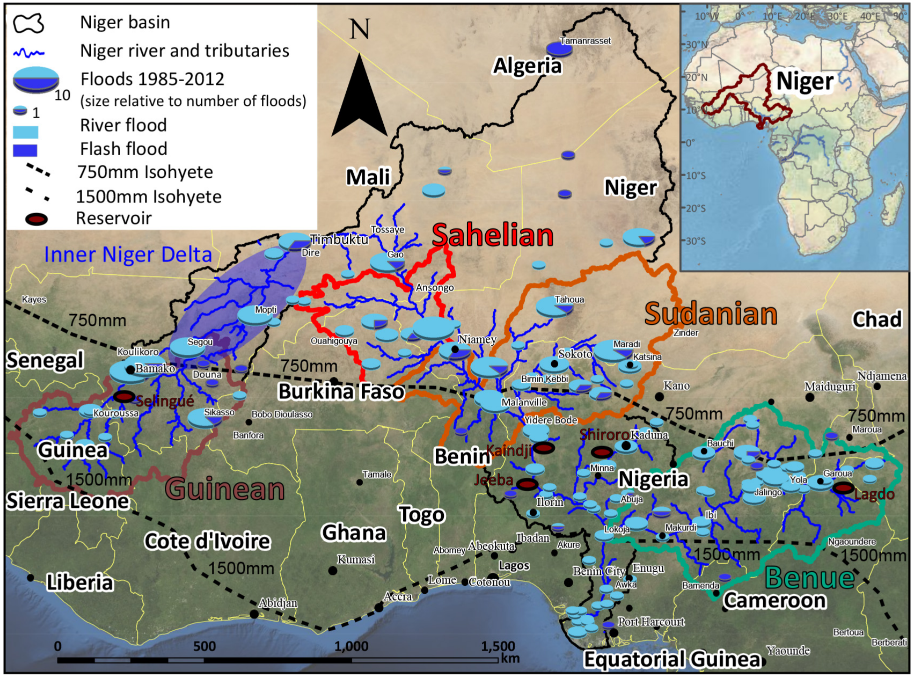

Figure 1. Niger basin and source areas of floods in the Guinean, Sahelian, Sudanian and Benue regions.

NHESSD
2, 5171–5212, 2014

Floods in the Niger basin – analysis and attribution

V. Aich et al.

Title Page
Abstract | Introduction
Conclusions | References
Tables | Figures
◀◀ | ▶▶
◀ | ▶
Back | Close
Full Screen / Esc
Printer-friendly Version
Interactive Discussion

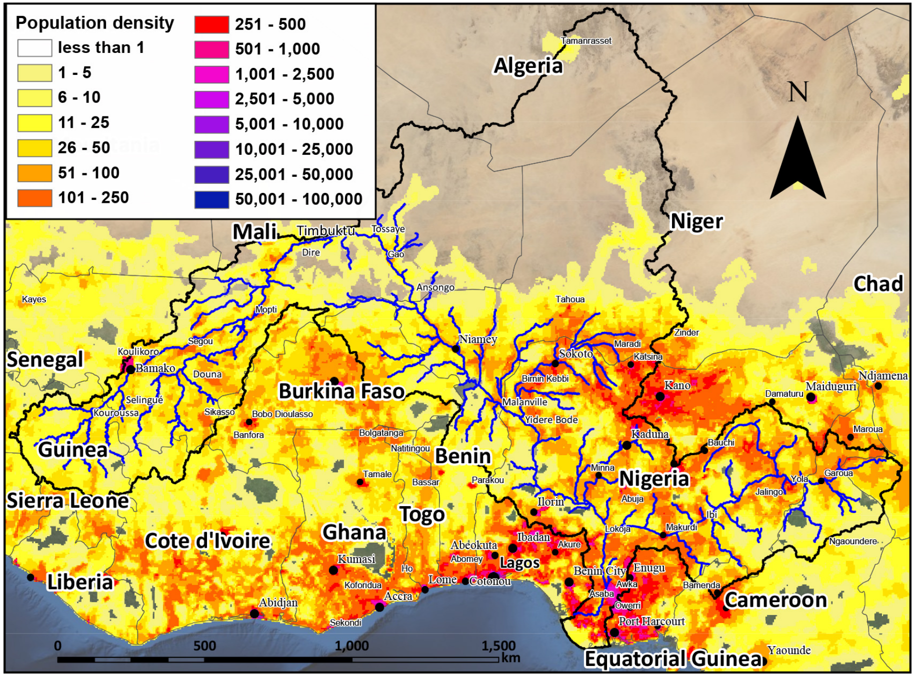

Figure 2. Population density in the Niger basin (data derived from Nelson, 2004).

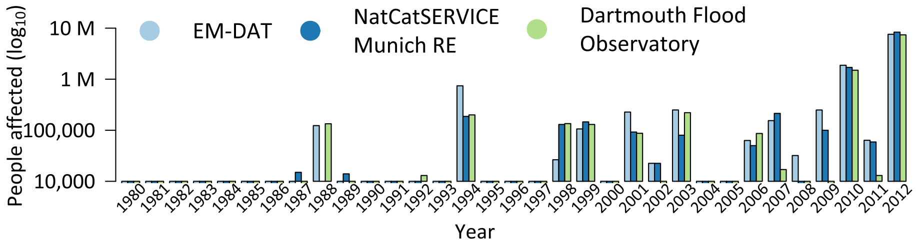

Figure 3. People affected by catastrophic floods per year in the Niger basin from 1985 to 2012 for three different data sources. Note that the scale of the *y* axis is logarithmic.

NHESSD
2, 5171–5212, 2014

Floods in the Niger basin – analysis and attribution

V. Aich et al.

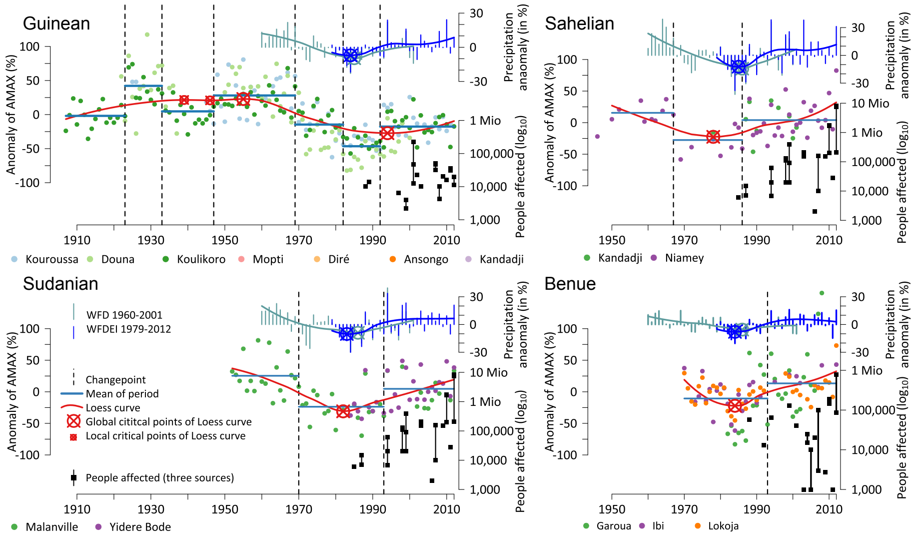

Figure 4. People affected by floods in the Niger basin, annual maximum discharge (AMAX) and precipitation separated for the four subregions. Note that the same numbers of affected people are plotted for the Sudanian and Sahelian regions (see Sect. 3.1.1). Detected changepoints for the mean AMAX in each region are plotted as black dashed lines.

NHESSD
2, 5171–5212, 2014

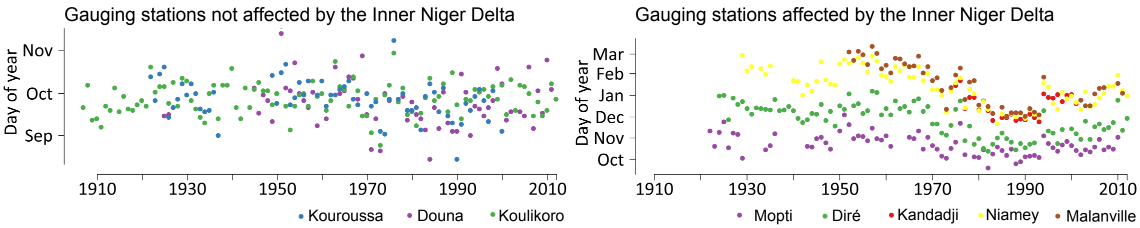

Figure 5. Shift in day of AMAX for the Guinean stations upstream of the Inner Niger Delta (left) and for the stations influenced by the Inner Niger Delta (right).

NHESSD
2, 5171–5212, 2014

Floods in the Niger basin – analysis and attribution

V. Aich et al.

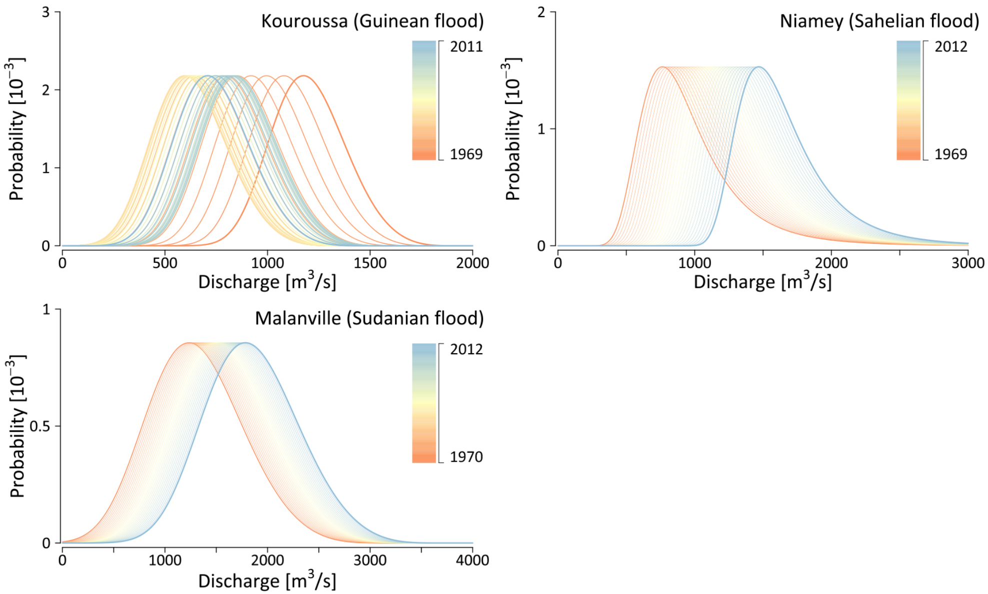

Figure 6. Non-stationary extreme value probability distributions for Kouroussa, Niamey and Malanville.

NHESSD
2, 5171–5212, 2014

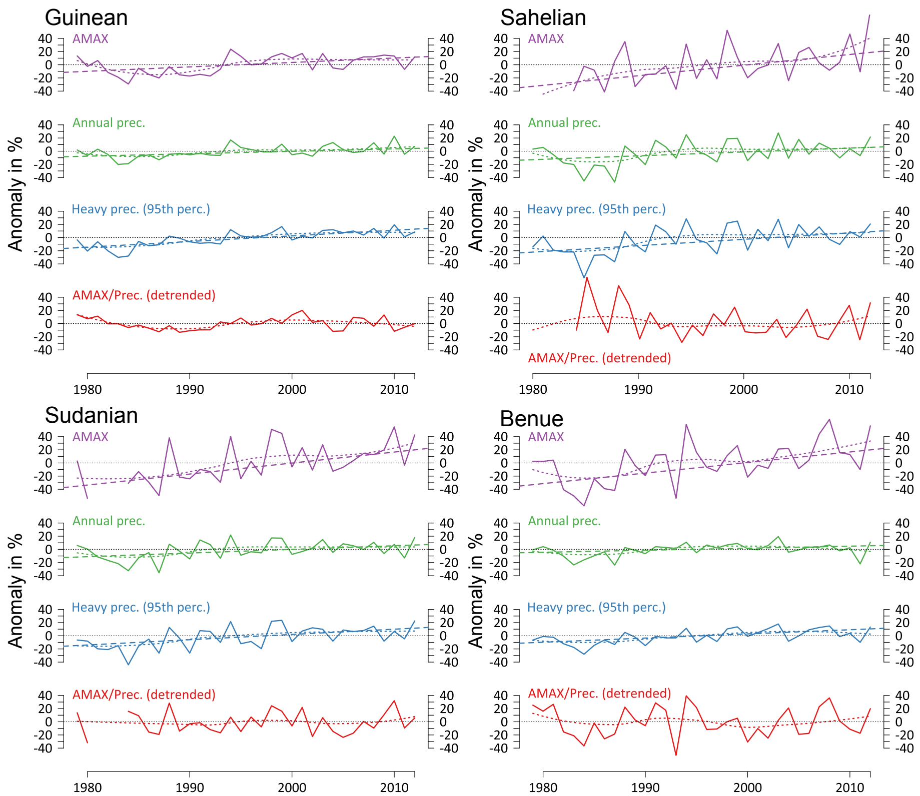

Figure 7. AMAX, annual precipitation, heavy precipitation and runoff coefficient (AMAX/Prec.) for the four subregions of the Niger basin as an anomaly, with Loess curve (dotted line). The Theil–Sen estimator trend is added as a dashed line when the Mann Kendall test was positive ($\alpha = 0.05$).

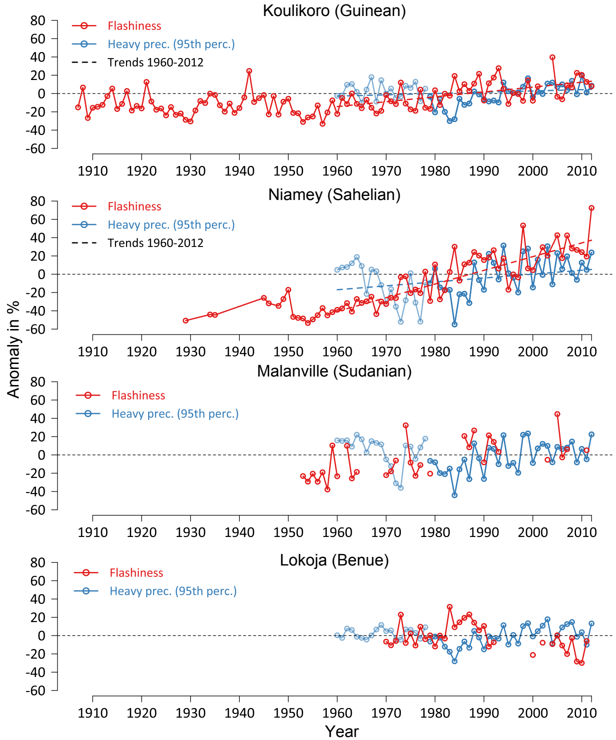

Figure 8. Anomaly of Richards–Baker flashiness index and heavy precipitation (95th percentile) for representative gauges in the Guinean (Koulikoro), Sahelian (Niamey), Sudanian (Malanville) and Benue (Lokoja) subregions. The normalization is based on the years 1960–2012 for which precipitation data is available. The Theil–Sen estimator trend is added as a dashed line for Koulikoro and Niamey. For Malanville and Lokoja, measurements are not sufficient to estimate the trend.

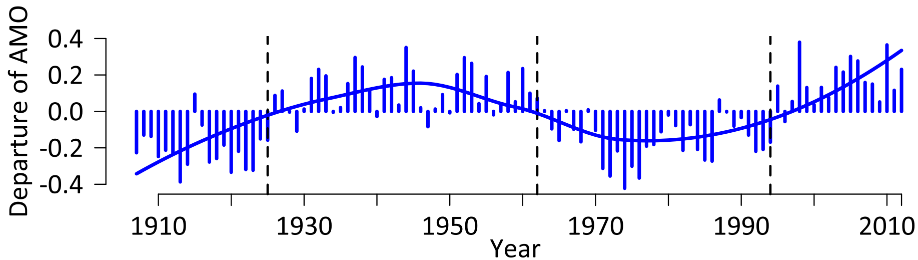

Figure 9. Atlantic Multidecadal Oscillation with LOESS curve as a blue line and detected changepoints as dotted black lines.

NHESSD
2, 5171–5212, 2014

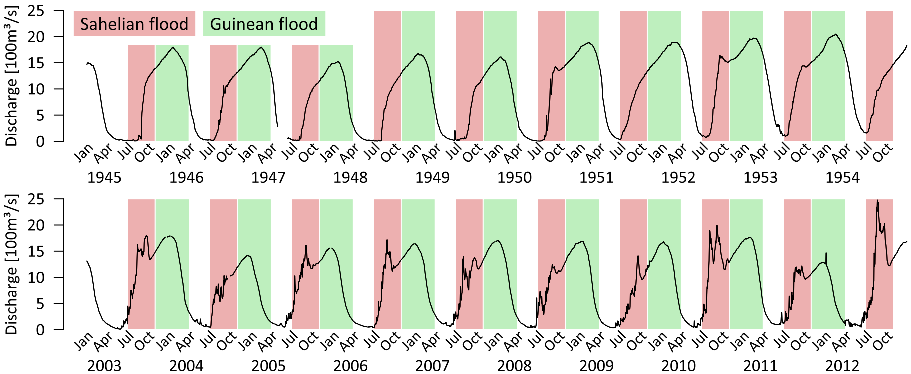

Figure 10. Hydrograph of the Niamey gauging station with Sahelian flooding (red) and Guinean flooding (green) for the period from 1945 to 1954 (dominant feature: single peak) and 2003 to 2012 (dominant feature: multiple peaks).

NHESSD
2, 5171–5212, 2014

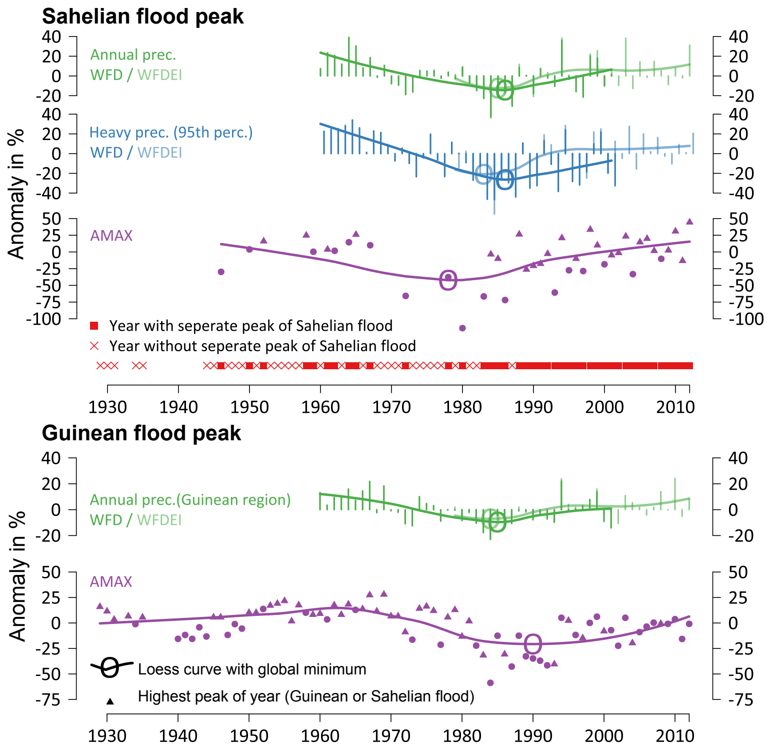

Figure 11. Top: Sahelian AMAX for the Niamey station and annual/ heavy precipitation from WFD and WFDEI for the Sahelian region. The red squares and crosses at the bottom of the upper figure mark years with and without separate peaks of Sahelian flooding. Bottom: Guinean AMAX for the Niamey station and annual precipitation from WFD and WFDEI for the Guinean region, all with Loess curves and global minima and as an anomaly in %.

NHESSD
2, 5171–5212, 2014

Floods in the Niger basin – analysis and attribution

V. Aich et al.

Title Page
Abstract Introduction
Conclusions References
Tables Figures
Back Close
Full Screen / Esc
Printer-friendly Version
Interactive Discussion